

A Segmented Beam Dump for the CTS Line at CTF3

M. Olvegård, W. Andreazza, E. Bravin, N. Chritin,
A. Dabrowski, M. Duraffourg, T. Lefèvre

May 10, 2012

Abstract

We propose a new segmented beam dump to be installed in the spectrometer line at the end of the CTF3 linac. The device will allow for time-resolved energy distribution measurements in a single shot and would therefore be a useful tool in tuning the accelerator.

1 Introduction

Segmented beam dumps have proved to be useful tools in the CTF3 operation [1]. Installed at the end of spectrometer lines [2], as depicted in Fig. 1(a), these devices provide energy distribution measurements with a time resolution of down to 5 ns in the current configuration. There are four segmented beam dumps installed so far. One is located at girder 4 just after the drive beam injector, and another one at girder 10, after the 8th accelerating structure [3]. A third device is installed in the PHIN spectrometer line [4] and a fourth, and the most recent one, at the end of TBL in CLEX [5]. All of these have been designed for their particular use and beam conditions, and have been installed and commissioned in stages.

In this report a fifth segmented beam dump is proposed. The device is a copy of the latest and most refined version [5], which is the one installed in TBL in 2011. We propose the installation of the new device in the spectrometer line in the CTS line, located between the Delay Loop and the Combiner Ring. A segmented beam dump in this location would complete the set of time-resolved spectrometry in the linac. Small energy variations along each beam pulse is important for a flat RF power production in CLEX. A small energy spread is also necessary for avoiding beam losses further down the complex. By changing the amplitudes and phases of the klystrons feeding the accelerator structures it is possible to adjust the energy spectrum of the beam. The segmented dumps at girder 4 and 10 are currently the only tools

to monitor the beam energy spectrum and energy spread energy resolved in time. With a segmented beam dump in the CTS line there would be a way to monitor the final energy distribution of the beam, before bunch frequency manipulations and power extraction.

Previously, another instrument has been used in this location. A Multi-Anode Photomultiplier Tube (MAPMT) detecting the light from an OTR screen in the spectrometer line was used for time resolved spectrometry [6]. This device, however, was subject to strong background noise that, despite several attempts, could not be shielded. The MAPMT is no longer in use but the equipment remains in place.

2 The Segmented Beam Dump

A segmented beam dump is a simple, robust and radiation-hard instrument. In this device the beam particles are stopped inside parallel metallic plates and the deposited charge is measured in the same way as in a Faraday cup. From each plate the beam-induced current flowing to ground through a $50\ \Omega$ resistance is detected and read by a fast acquisition channel. See Fig. 1(b) for a sketch of the system. A water-cooled collimator, visible in the sketch in Fig. 1(a), is placed in front of the detecting segments. The collimator lets a small fraction of the beam pass through to the segments through thin slits, one slit per segment. It acts as a thermal buffer for the system by absorbing most of the beam power. Even though most of the particles are filtered out by the collimator, the signal to noise ratio of the segmented dump is very good due to the high intensity beam at CTF3.

Table 1: Characteristics of the segmented dump in TBL.

Part	Dimension		Materials
Segment	width	3 mm	Tungsten
	height	60 mm	
	length	20 mm	
Insulator	width	1 mm	Alumina
	height	10 mm	
	length	20 mm	
Collimator	length	100 mm	Inermet ¹
	slit width	0.4 mm	

¹ Commercial compound with high tungsten content [8].

A few modifications to the original segmented dump system was made for the installation in TBL. Firstly, extensive simulations were made in or-

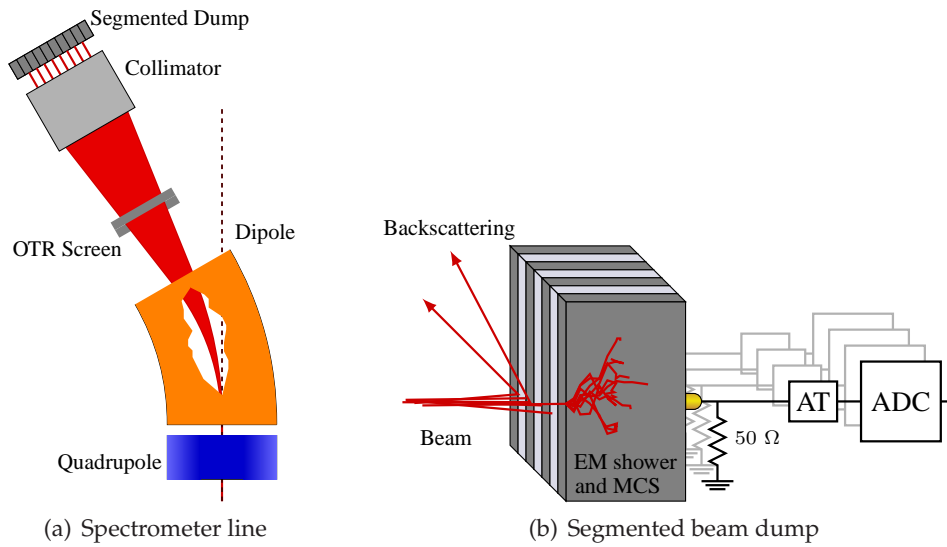


Figure 1: A sketch of a segmented beam dump installed in a spectrometer line (a) and a close-up on the basics of the detector (b).

der to optimize the system for the expected beam conditions (see [5] for details). The result is presented in Table 1. Secondly, more attention was paid to the long-term robustness of the system and to a possible upgrade to a faster acquisition channel. Third: from operational experiences it had been understood that a shift to a new detector geometry would be necessary. This shift means to go from a geometry where the segments and the collimator slits are placed parallel to the spectrometer axis, to a “concentric” geometry where the slit and segment positions match the divergence of the beam after passing through the dipole magnet. This modification increases the angular acceptance of the detector and ensures a uniformity in response of the segments. Figure 2 presents sketches of the two different configurations. See [7] for more information on how the non-uniformity was quantified and corrected in the CTF3 linac.

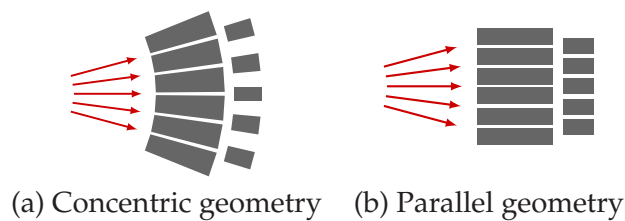


Figure 2: Two different detector geometries. The concentric geometry (a) improves the response of the detector and has been implemented in the TBL segmented dump. Note that the angles are strongly exaggerated.

While the long-term survival of the device will take longer to evaluate, the result of the geometry change was investigated during the commissioning of the segmented dump in TBL. Figure 3 shows the measured response of each segment, normalized to the maximum response. The response has been extracted from a dipole scan measurement, where the beam is steered across the detector in small step by slowly increasing the dipole current. Each segment is used to scan through the beam profile and the spectrum is integrated over a selected time window. The peak of this projection is taken as the segment response. The same figure also contains the equivalent response curve of the segmented dump at girder 10, which has the former parallel detector geometry. The improvement in uniformity is clear. Note that the sharp decrease of the response at ± 50 mm comes from the fact that the last piece of vacuum chamber in TBL limits the acceptance of the measurement.

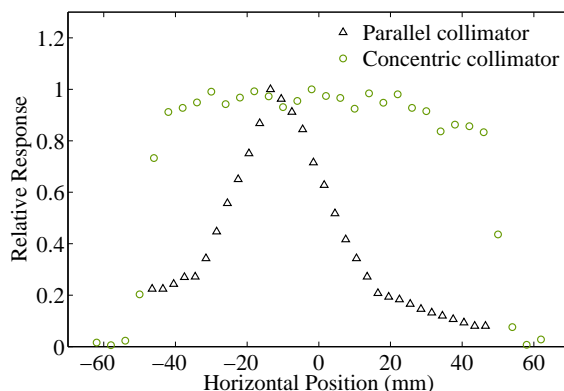


Figure 3: Response curve of segmented beam dumps of two different generations: TBL with concentric detector geometry and spectrometer 10 with parallel detector geometry.

2.1 Necessary modifications

The most crucial point for directly adapting the new segmented dump design to the suggested location is the geometry: The “focal point” of the concentric slits need to be at the center of the bend. Luckily, the beam dump in the CTS spectrometer line is located at a distance from the spectrometer magnet CTS.BHB0800 that fits the TBL design almost perfectly. This allows us to keep the 2000 mm bending radius. However, the last piece of vacuum chamber reaches into the beam dump. In order to make room for a segmented dump this requires a modification; either shortening the existing vacuum chamber or manufacturing a substitute.

To design and build a new beam dump would be needed in order to fit in the new detector. An exit canal is needed for the semi-rigid cables that brings the signals from the segments out of the beam dump. This also means that the existing beam dump must be disassembled. Naturally, a thorough radiation survey would have to take place before any disassembly can take place.

During the installation of the segmented dump in TBL we gained some experience that will be useful now. The printed circuit board for signal readout (PCB) in the original design was made on a ceramic plate. The reason to have a ceramic (alumina) plate was to have a readout system that would be as radiation hard as possible. This plate was mechanically damaged during the preparation (alumina is brittle) and another solution had to be found. With small modifications to the shape of the plate we hope to avoid these problems.

Furthermore, the full PCB assembly, with contact pins and semi-rigid cables, turned out to be more fragile than expected. More generous space for the soldering and an extra support for the card assembly that would fix it more firmly to the rest of the assembly, is expected to overcome this problem.

When CTF3 is operated at higher repetition rates the thermal load increases significantly. The TBL segmented dump is equipped with a water-cooled collimator. Up to 5 Hz repetition rate the maximum temperature of the collimator stays safely below any risk of thermal damages. Water cooling is recommended also for the new segmented dump and a water connection nearby needs to be foreseen for this.

Note, though, that there are already 32 available ADC channels, belonging to the MAPMT, with cables between the ADCs and the detector location. This reduces the installation costs significantly.

3 Expected performance

With the present configuration, with an ADC channel sampling the signal from each individual segment, the time resolution is limited by the sampling rate of the ADCs. With other acquisition methods a time resolution down to 0.5 ns is possible [4]. The ADCs that were used for the MAPMT are of the same type as those used for the segmented beam dumps in the CTF3 linac, i.e. SIS 3300 with 100 MS/s. This means a time resolution of approximately 10 ns which is enough to see the energy variations along each pulse with a sufficient temporal granularity.

The spatial resolution and also the energy resolution is dominated by the detector granularity, i.e. the spacing between plates. This granularity has been optimized for the nominal beam in TBL after deceleration in several PETS [9]. The maximum energy of the TBL beam is the same as the beam energy after the final accelerating structure. The biggest difference between the beams is the expected energy spread. While in TBL single-bunch energy spreads of up to 6% can be expected, the equivalent value in the CTS line is around 1%. Note, though, that the central spectrometer angle is 22.5° in the CTS spectrometer line, which is 2.25 times larger than the angle of the TBL spectrometer line. Since the same type of dipole magnet is used that means roughly a 2.27 times larger dispersion, $D = 0.7$ m.

The transverse resolution of the segmented dump in TBL has been estimated both through simulations and through measurements. The detector geometry was inserted into FLUKA [10, 11], a Monte Carlo simulation code. An electron beam with a very small cross section compared to the width of a segment was used to estimate: a) the signal spill from crosstalk caused by scattered particles; b) the increase of the beam size from scattering in thin foils in the beam line, i.e. the OTR screen and the vacuum window. The former (a) was checked by studying the net charge stopped in every segment when the beam is hitting only the middle segment. The minimum beam size measurable can be obtained from these simulations. At a beam energy of 150 MeV these two effects are expected to give a contribution of $\sigma_{crosstalk} = 2.7$ mm and $\sigma_{scattering} = 1.7$ mm to the measured beam size. Adding these in quadrature gives the minimum resolution: $\sigma_{res} \geq 3.2$ mm which for TBL is equivalent to a resolution on momentum spread of 0.9%.

An OTR screen in the TBL spectrometer line (see Fig. 1(a)) was used for cross-calibration of the segmented beam dump and to measure the resolution. A beam of small energy spread was used and the optics was adjusted to have a beam waist in the spectrometer line. First, the Twiss parameters were measured at an OTR screen for transverse beam profile measurements just upstream from the spectrometer magnet. The result from these measurements were used to estimate the beta function both at the spectrometer screen location and at the segmented dump position. These numbers were then used for adjusting the beam size measurement in the spectrometer line, σ_{meas} , since the momentum spread is extracted from the relation in equation 1:

$$\sigma_{meas} = \sqrt{\varepsilon\beta_x + \left(D_x \frac{\Delta p}{p}\right)^2} \quad (1)$$

The beam profile was then measured simultaneously with the two devices and the corresponding energy spread calculated. The OTR screen was expected to give a more accurate result on the energy spread, given that the resolution of the screen is much better. The cross-calibration then gave a resolution of 1% for the segmented dump, which is very close to what was expected from simulation.

The dispersion at a segmented dump in the CTS line is approximately 2.25 larger than in TBL. With an identical detector geometry this means that the energy resolution expected from simulation would be 0.4%. If we use the measured resolution of 1% as a reference, then 0.44% would be the resolution on energy spread in the CTS line. For a nominal 1σ energy spread of 1% that would imply 2.25 measurement points per sigma in the beam profile. For Gaussian profiles this sampling density is enough to reproduce the profile within an error of $< 1\%$ [12]. With 32 channels the detector has a total horizontal size of approximately 13 cm. At 1% energy spread that gives an acceptance of 18σ .

Systematic effects, such as an increase in beam size from scattering in the OTR screen and the vacuum window, can be corrected. Such corrections, that can be easily computed through a series of simulations, would be particularly important at small energy spreads.

4 Conclusion

We have here presented a proposal to install a segmented beam dump of the TBL model in the CTS line. A segmented beam dump in this location will be the ideal tool for monitoring the final beam energy distribution at the end of the linac. Currently, the effect of RF phase and amplitude adjustments can only be confirmed up to half of the acceleration and a measurement at the end is needed for final tuning of the CTF3 linac, before sending the beam off for experiments. In TBL this device has displayed a good response uniformity, a 1% resolution on energy spread and 5 ns temporal resolution. Similarities between the two beam lines makes the adaptation of the system to the CTS line fairly simple. By using the dispersion in the CTS spectrometer line and the resolution of the device as confirmed by measurement, we expect an energy resolution of approximately 0.4%. The time resolution will be 10 ns, if already existing ADCs are used, but with a possible upgrade to better time resolution.

Acknowledgments

We wish to acknowledge the support of the CTF3 operation team and the CTF3 collaboration for construction and support. Thanks to Volker Ziemann who was kind enough to assist in the editing of this report. A special thanks also to Daniel Egger for excellent graphics and fruitful discussions.

References

- [1] A. Dabrowski *et al.*, in Proceedings of LINAC, Victoria, 2008, p. 585.
- [2] T. Lefèvre *et al.*, in Proceedings of EPAC, Edinburgh, United Kingdom, 2006, p. 1205.
- [3] T. Lefèvre *et al.*, in Proceedings of DIPAC, Venice, 2007, p. 340.
- [4] D. Egger *et al.*, in Proceedings of DIPAC, Hamburg, Germany, 2011, p. 431.
- [5] M. Olvegård *et al.*, in Proceedings of IPAC, Kyoto, Japan, 2010, p. 1113.
- [6] T. Lefèvre *et al.*, in Proceedings of EPAC, Edinburgh, 2006, p. 1205.
- [7] M. Olvegård, Master Thesis, Gothenburg University, Gothenburg, Sweden, January 22, 2009.
- [8] “Densimet[®] and Inermet[®] Tungsten Alloys”,
<http://www.plansee.com/lib/SD-DI-02.pdf>,
accessed: 2012-01-17, 15:00.
- [9] S. Döbert *et al.*, in Proceedings of LINAC, Tsukuba, Japan, 2010, p. 85.
- [10] G. Battistoni *et al.*, in Proceedings of the Hadronic Shower Simulation Workshop, Batavia, U.S.A, 2006, (AIP Conference Proceeding 896, 2007), p. 31.
- [11] A. Fasso *et al.*, CERN Report No. CERN-2005-10; INFN Report No. INFN/TC.05/11; SLAC Report No. SLAC-R-773, 2005.
- [12] E. Bravin, AB-Note-2004-016 BDI, Geneva, 2004.